The 2009 IEEE/RSJ International Conference on
Intelligent Robots and Systems
October 11-15, 2009 St. Louis, USA

Variable Impedance Magnetorheological Clutch Actuator and Telerobotic Implementation

Daniel S. Walker, Dan J. Thoma, and Günter Niemeyer

Abstract— **Variable impedance actuation is characterized by the ability to independently set output force and output impedance for a robotic device. Adjusting the output impedance in real-time allows a device to better adapt to a variety of tasks, operate in human-like fashion, and support human safety. This paper focuses on a Series Clutch Actuator based on magnetorheological fluid which allows a fast, electrical change of the impedance while maintaining good force tracking. In particular the mechanical clutch can alter the high-frequency impedance, decoupling the motor inertia and thus reducing impact forces. We present the mechanical clutch design and a control system architecture to automatically adjust the fluid magnetization level and leverage the clutch benefits. Experiments verify torque tracking and impact force reduction both in autonomous and telerobotic operation. The actuator was designed and manufactured in collaboration with the Materials Design Institute at Los Alamos National Laboratory, and is tested in a single degree of freedom demonstration.**

I. Introduction

As robotic applications extend beyond the industrial setting, operations in unstructured environments as well as interactions and collaborations with humans become more common. The physical characteristics of the robot-environment interface determine the nature of these interactions. A compliant interface reduces impact forces and adds safety for the environment, human, and device itself[1]. Stiff interfaces can provide greater bandwidth, smaller position error, and more safely support large forces.

Variable impedance actuators can potentially adjust a robot's characteristics to task and safety requirements in real-time. We distinguish the low-frequency impedance, which may be modulated by closed loop control, from the high-frequency impedance, which falls above the bandwidth of any controller. In order to alter the high-frequency impedance, which can be used to reduce impact forces, physical adjustments are necessary.

Beyond enhancing safety, variable impedance has the potential to bring human-like manipulation to telerobotics. Much as contraction of antagonistic muscle pairs changes the impedance of a human limb, the slave can act better as a stand-in for a human operator by either automatically or explicitly adjusting its impedance.

This work was supported by the Materials Design Institute at Los Alamos National Laboratory and by the National Science Foundation

D.S. Walker is with the Department of Mechanical Engineering, Stanford University, Stanford, CA 94035, USA daniel.walker@stanford.edu

D.J. Thoma is with the Materials Design Institute, Los Alamos National Laboratory, Los Alamos, NM 87545, USA thoma@lanl.gov

G. Niemeyer is with the Faculty of Mechanical Engineering, Stanford University, Stanford, CA 94035, USA gunter.niemeyer@stanford.edu

In this work, we achieve variable impedance through the addition of a series clutch element based on magnetorheological fluid (MRF)[2]. MRFs can change behavior in the presence of a magnetic field in tens of milliseconds, creating the potential for real-time adjustment of the physical coupling between actuator inertia and end effector. This affects high-frequency impedance characteristics similarly to Series Elastic Actuators (SEA)[3].

Previous work with MR clutch-modulated actuators has focused on servoing the magnetic field in the fluid to produce a desired torque or to track a desired viscous impedance. Since the speed of the servo limits the frequencies over which actuator impedance can be altered, we propose in this work to use a motor to regulate output torque and the MRF magnetization in the clutch to alter the mechanical coupling between actuator and output. This enables torque tracking while independently controlling output impedance.

We first explore the general options for adjusting output impedance and then briefly review the design of the clutch. Next we discuss the control architecture, driving the motor, regulating the clutch's electromagnetic coil current, and a complete 1-DOF telerobotic system. In experiments we verify the actuator's torque tracking capabilities, impact force reduction, and the applicability of our design to teleoperation.

II. Background

Most robotic devices connect their actuators via transmissions and linkages to an end-effector, which interacts with the world. The output impedance

$$Z(s) = \frac{F}{v} \tag{1}$$

is the transfer function of velocity to force and describes how the device feels, e.g. to a user holding and pushing on the end effector. The natural impedance of an actuator is modeled in Figure 1 as a direct connection between actuator and output. At low frequencies the natural device impedance is dominated by friction, and at high frequencies by the total mass, as shown in Figure 2 and Figure 3.

A. Feedback Control

Active controllers can affect the impedance of a device through feedback control. In particular, stiffness controllers use a PD to regulate the device output to a setpoint via an artificial spring/damper, increasing the low-frequency impedance. We plot the device impedance under stiffness control in Figure 2.

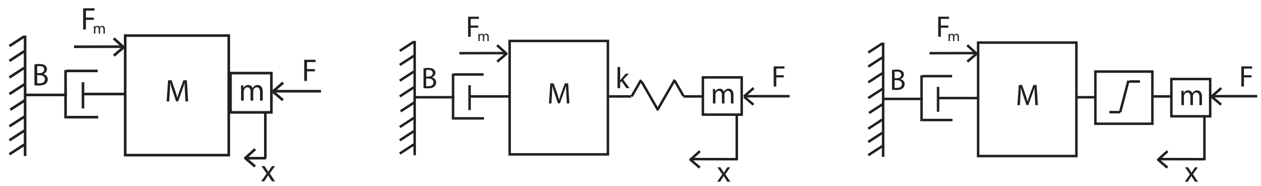

Fig. 1. Lumped Parameter Model of Direct Actuator-Output Connection, SEA, and SCA

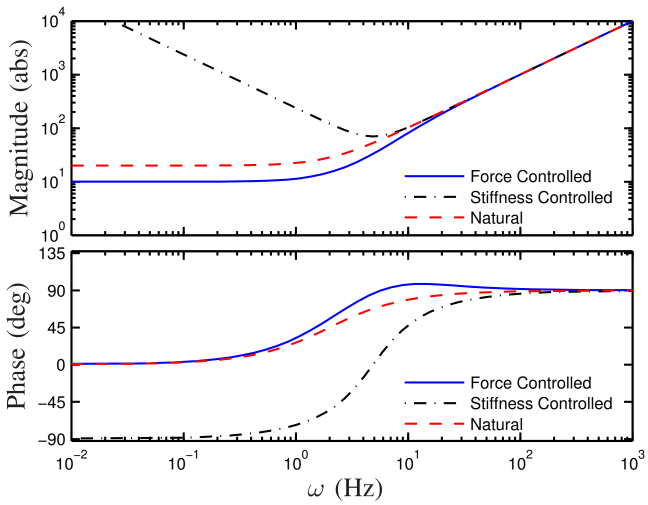

Fig. 2. Feedback Control Alters Only the Low Frequency Impedance

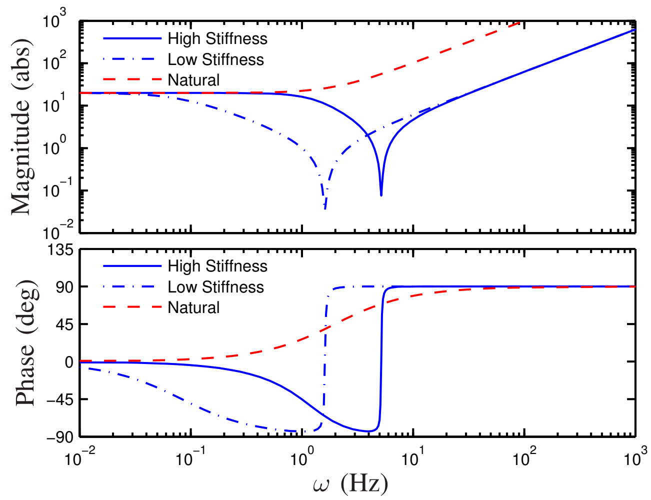

Fig. 3. Series Elastic Actuation Mechanically Decouples the Actuator Mass at High Frequency

Force controllers act to reduce apparent friction and mass. However, due to limited control bandwidth from non-colocation of the actuator and force sensor, amplifier dynamics, and sensor rolloff, the system will retain its natural high-frequency impedance. In general, any control method will be unable to affect the device impedance at high frequency due to these effects. Such controllers will also result in non-passivity due to the introduction of phase above $90°$.

B. Mechanical Couplings

The high-frequency impedance is an important characteristic for human safety in the context of collisions and impacts. Impacts give rise to sudden changes in velocity and dangerously large interaction forces. These impacts last up to tens of milliseconds so that the impedance at frequencies of tens and hundreds of Hertz can be used to predict the magnitude of impact forces. Effectively this high-frequency impedance is dominated by the device mass. Several design methods introduce a mechanical coupling between the actuator and output linkage in order to decouple the actuator from the output, masking the actuator inertia. As an example, SEA adds an elastic component between the motor and the end effector, which reduces impedance and force bandwidth[3]. A model of an SEA system is provided in Figure 1.

The impedance of the SEA device is plotted in Figure 3. Two values of the spring constant are shown to demonstrate the effect of changing elasticity. We see the high-frequency impedance is dominated by the low, decoupled output mass. Additionally, lowering the series stiffness lowers the transition frequency, hiding inertia over a larger range of frequencies but lowering the possible force control bandwidth. In general, a physical coupling must be inserted between actuator and output to affect high-frequency impedance.

In addition to SEA, there are a range of actuator designs which use mechanical couplings to alter high-frequency impedance. Series Damper Actuators (SDA)[4] are capable of similarly affecting the high-frequency device impedance by inserting a damper between the actuator and output. Several developments are creating mechanically variable series compliances to further alter the couplings in real-time and achieve a range of output impedances[5], [6], [7]. MRFs have also been used as a mechanical coupling to adjust impedance, as in tunable prostheses[8], [9], human safe compliant joints[10], and human safe interlocks[11]. The MRF has also been employed specifically in clutch-style actuators by[12], [13], [14].

III. Magnetorheological Series Clutch Actuator

Due to the inability of control methods to affect high-frequency impedance, a variable impedance actuator capable of changing high-frequency impedance must contain a mechanically variable impedance. In order to realize such an

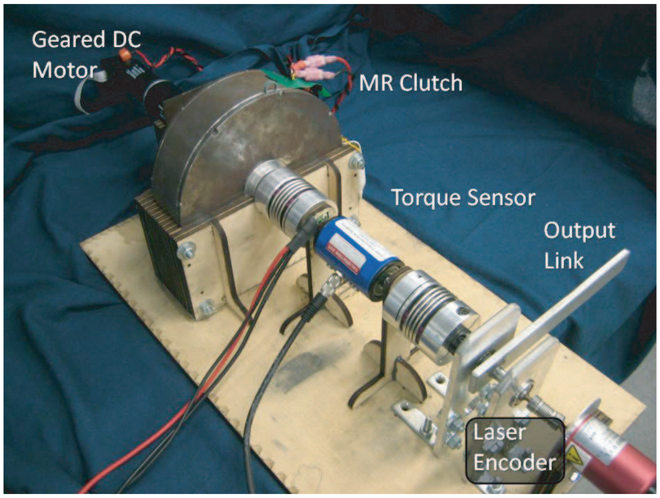

Fig. 4. Prototype SCA System

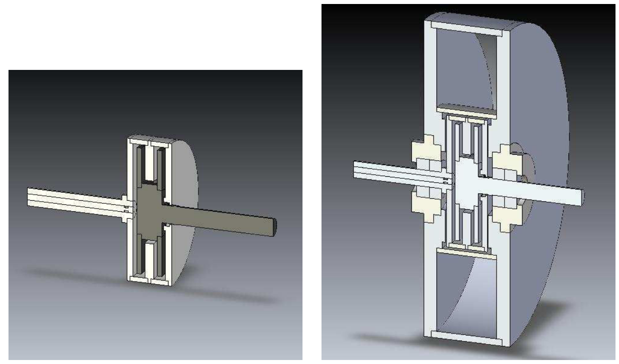

Fig. 5. Clutch Design: Torque Transfer Drum with Parallel Plates and Cross Section of Clutch Assembly Encasing Drum

actuator, we designed and manufactured a clutch using MRF to transfer torque between a series of a parallel plates.

A. Variable Impedance Series Clutch Actuation

A Series Clutch Actuator (SCA) utilizes a clutch between the motor and output, which transfers torque up to some saturation level, as shown in Figure 1. In our SCA, the torque saturation level is determined by the magnetization of the MRF, allowing the saturation level to be altered in real-time during clutch activity.

If the saturation level is chosen to be very high, the natural device impedance is recovered. If the saturation is set to the actuator's maximum torque requirement, all motor torque will be transmitted while large impact torques will be masked. If it is set low, the clutch will transmit only minimal torques subject to a small residual viscosity. Due to this saturating nature of the torque transfer, the impedance of the SCA is magnitude-dependent, and thus nonlinear.

While a series clutch can alter the output impedance, it does not add dynamic elements between the actuator so that the achievable force control bandwidths remain unchanged.

Our 1-DOF prototype actuation system is shown in Figure 4. A Maxon RE35 with 74:1 gear reduction and an encoder are attached to the clutch input shaft. A Cooper LXT 971 torque sensor, 17 cm handle link and Canon laser encoder are attached to the output shaft. The motor and the clutch coil currents are both regulated using Copley 412 amplifiers and a 75 V Copley power supply.

B. Magnetorheological Fluid

MRF is a suspension of ferrous particles in an oil-based solution. Under the presence of a magnetic field, the ferrous particles align themselves into chains which drastically alter the rheology of the fluid. This organization takes on the order of 10 ms to occur, according to information from LORD Corporation. The varying fluid properties may be utilized to transfer torque in several different modes: shear, valve, and squeeze[2]. Typically, the behavior of an MRF is modeled with the Bingham-Plastic model[15].

C. Clutch Design

Our clutch uses two parallel output plates, shown in dark in Figure 5, to limit radial size. A plate radius of 33.65 mm was selected using the torque equations of [14]. The MRF between the plates transfers torque in shear mode. The input (light) and output (dark) shafts were mounted in bearings and installed in an outer casing to house the electromagnetic coil and provide a flux path through the fluid. This coil has an experimentally determined inductance of 9.72 H and a resistance of 108 Ω, with a time constant of 90 ms.

Both the air gap around the torque transfer drum and the fluid gap between the internal plates resist the flux[13] and were minimized to 0.5 mm and 1.9 mm, respectively, to improve magnetic field strength. Additionally, the thickness of the plates comprising the outer casing was selected to avoid saturation. The overall clutch case radius is 91.5 mm.

The clutch's input and output have inertias of 2840 gcm^2 and 850 gcm^2, respectively. In contrast, the motor's reflected rotor inertia is 359000 gcm^2. In our completed system, the approximate inertia of the output stage is 7500 gcm^2 while the approximate inertia of the input stage and motor is 370000 gcm^2, allowing 98% of the system inertia to be decoupled from the output.

D. MR Clutch Performance Characteristics

Unfortunately, MRF does not transfer torque viscously in shear mode. As input velocity changes, the output torque increases quickly and then practically saturates; further increases in velocity lead to very small increases in torque. As a magnetic field is applied, this saturation level increases, as shown in Figure 6. These results were obtained by locking the output of the actuator and varying the speed of the input shaft at a constant coil current.

Adding further complication, ferrous particles in the MRF and steel casing cause a hysteresis between applied magnetic field and fluid magnetization. Figure 7 demonstrates this as a hysteresis between the coil current and transferred torque. The data was obtained by locking the output shaft and

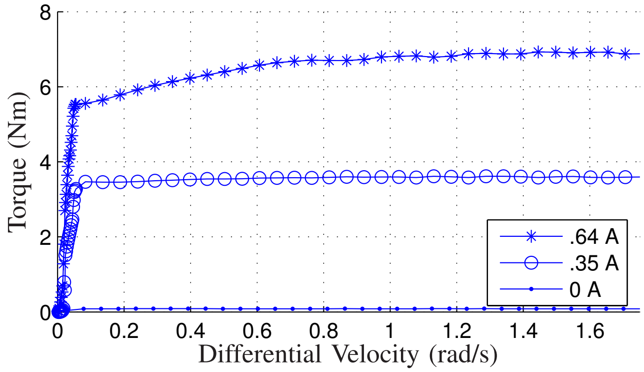

Fig. 6. Saturating Nature of the Torque Transfer in the MR Clutch

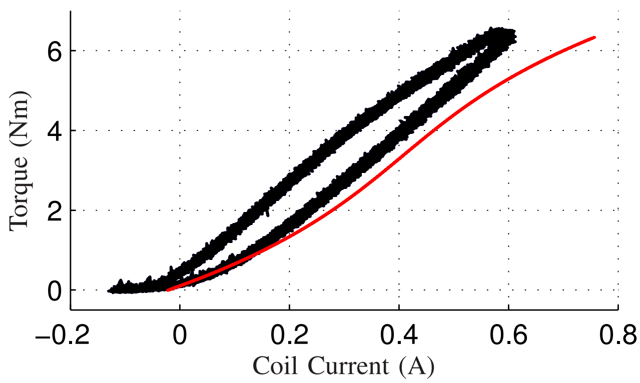

Fig. 7. Hysteretical Torque Transfer and Conservative Selection of Current Needed for a Desired Torque

rotating the input shaft at a velocity of 1.5 rad/s. Due to the hysteresis, a slightly negative current is necessary to destroy the magnetization of the ferrous materials and achieve zero magnetic field in the fluid. Accordingly, in order to return to a low impedance from a high impedance, it may be necessary to utilize negative current.

IV. SCA Controller Architecture

The two SCA inputs, motor torque τ_m and coil current i_{coil}, determine the output torque τ and clutch saturation level. The two inputs allow, in principle, separate control of both the output force and impedance. Therefore a control architecture should be selected which retains this ability.

In selecting a controller architecture for the SCA, we consider the output torque responses shown in Figure 8 to separate steps in motor current and clutch current. The slow 90 ms time constant of our coil limits the torque rise time in response to clutch activation.

Due to the faster rise time of the motor dynamics and the motor's inability to affect the high-frequency impedance, we propose a control architecture using the motor to regulate torque and the electromagnetic coil to regulate impedance.

Unlike previous approaches with MR clutches, we do not attempt to feedback-linearize the MRF's non-viscous behavior or regulate the MRF from torque sensor readings.

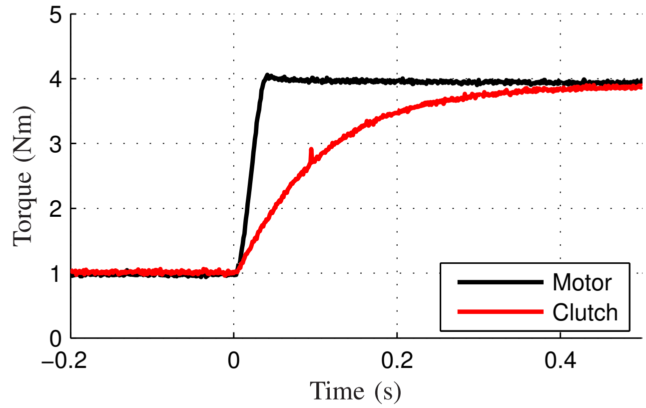

Fig. 8. Rise time of Torque Transfer Using a DC Motor or Coil Current

This choice best utilizes the SCA's capability to alter the high-frequency impedance beyond the bandwidth of active feedback, though it prevents a complete linear analysis.

A. Torque Controller

A torque controller was created for the SCA using explicit feedback from the sensed output torque τ and motor velocity $\dot{\theta}_m$. Contact instability was addressed with a lead compensator, and steady state torque error was improved with a lag.

$$\tau_m = \tau_d + K(s)(\tau_d - \tau) - k_v \dot{\Theta}_m \tag{2}$$

$$K(s) = 16\,\frac{s + 72.26}{s + 289}\,\frac{s + 9.425}{s + 3.77}$$

$$k_v = 0.35 \text{ Nm/(rad/s)}$$

B. Clutch Electromagnetic Coil Current Controller

The coil current is controlled with the goal of automatically regulating the torque saturation level and consequently the high-frequency impedance. In these initial experiments, the impedance was regulated to the minimum capable of transmitting the desired torque. However, other controllers are envisioned which regulate the impedance to meet other objectives, such as matching a user's impedance.

To ensure sufficient MRF activation, we apply a coil current equivalent to the maximum current required for 120% of desired torque. The commanded current is then

$$\begin{aligned} i_{coil} = {} & 0.0020(1.2\tau_d)^3 - 0.0243(1.2\tau_d)^2 \\ & + 0.1713(1.2\tau_d) - 0.0207 \end{aligned} \tag{3}$$

where the maximum current was fit by a cubic polynomial. This torque to current relationship is shown in Figure 7.

C. Combined Telerobotic Control Architecture

The SCA was also implemented in a telerobotic system as shown in Figure 9, comprised of the two SCA controller components discussed above and a PD controller to link master and slave.

This PD controller uses the relative position and velocity of the slave output and master device to calculate a desired

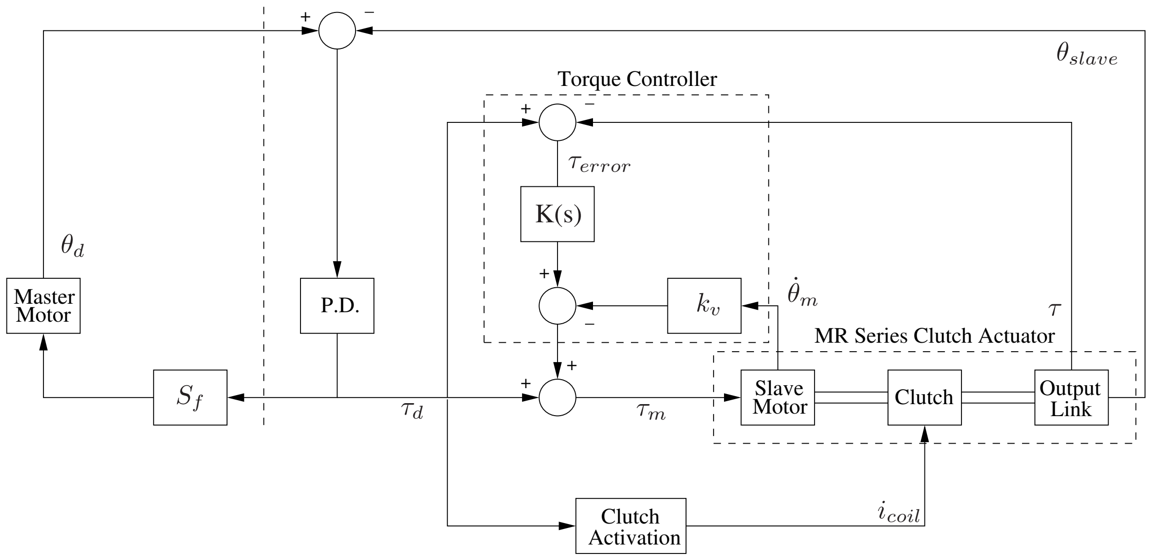

Fig. 9. Motor and Coil Control Architecture for Tracking Torque while Minimizing Impact Forces

torque τ_d. On the master this torque is scaled and applied to the user via a motor. On the slave the desired torque is used as the reference signal to the torque controller. Additionally, the desired torque is fed forward through the 1.2 gain and polynomial to set the commanded coil current of the clutch. These two controllers work together to transmit the desired torque at a conservatively chosen minimum impedance. This ensures that unexpected collisions will not result in larger impact torques than the commanded torque.

V. SCA EXPERIMENTS

Four experiments were performed to demonstrate the capabilities of the SCA system. The first shows SCA torque tracking against a rigid environment independent of clutch activation. The second shows correlation between the magnitude of impact torques and the clutch activation level, i.e. the ability of the SCA to set high-frequency impedance. The third demonstrates automatic control of the clutch impedance. The fourth experiment tests the ability of the SCA to track desired position and force in a telerobotic system while automatically reducing impact forces in collisions.

The first two experiments utilize three levels of clutch impedance by directly commanding currents to the clutch coil. High, medium, and low used 0.64 A, 0.35 A, and 0.0 A to set saturation levels of approximately 6.5 Nm, 3.5 Nm, 0 Nm, respectively. A clutchless, direct coupling was also tested by replacing the clutch with a rigid steel shaft.

With the clutch removed, the torque controller was slightly retuned for the removal of the clutch inertia to:

$$K(s) = 18\ \frac{s + 87.96}{s + 351.9}\ \frac{s + 9.425}{s + 3.77}$$

$$k_v = .15 \text{ Nm/(rad/s)}$$

Additionally, in telerobotic experiments without the clutch, the same architecture was used as in Figure 9 without the coil current controller and with a direct connection between slave motor and output link.

A. Torque Tracking

The output link of the system was locked, and output torque steps from 1 Nm to 3 Nm were commanded in order to ensure environment contact was maintained during the experiment. Figure 10 shows the resulting step responses.

We notice that the presence of the clutch has a negligible effect on the dynamics of the response. As expected, the unactivated case cannot track the desired torques, as its saturation level is below 1 Nm.

B. High Velocity Collisions

High speed impacts (6.5 rad/s or 1.1 m/s at the end effector) were performed with our end effector through the variable impedance SCA at three levels of clutch activation and with the SCA removed. The resulting impact torques are plotted in Figure 11.

We see that lowering the device impedance via the coil current has reduced the impact torque. The SCA lowers the high-frequency impedance below natural levels. Even with the clutch fully activated, the peak torques experienced are much smaller than with the rigid coupling. The effect becomes more prominent with a reduction in clutch activation.

Integrating torque during the collisions without the clutch and with the clutch low, we note that the angular momentum absorbed in the impact has decreased from 0.280 Nms to 0.0065 Nms, a factor of 43. These numbers are in good agreement with the approximate values of the system output inertia (7437 gcm^2), the large reflected motor inertia (359000 gcm^2), and their ratio at 48.3.

C. Controller Regulation of Clutch Electromagnetic Coil Current

A desired torque of 3 Nm was commanded to the SCA at rest out of contact, causing the device to accelerate before

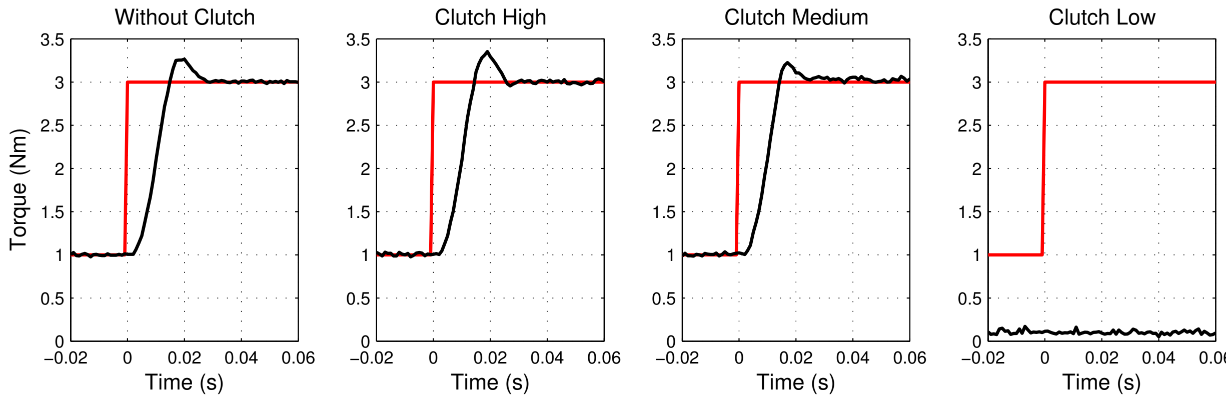

Fig. 10. Torque Tracking under Varying Clutch Impedance

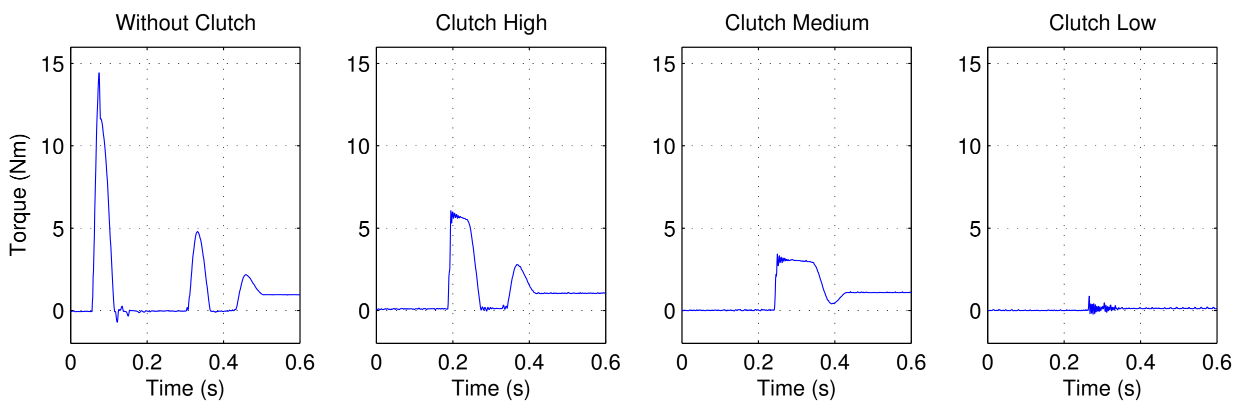

Fig. 11. 6.5 rad/s Collision Impact Torques under Varying Clutch Impedance

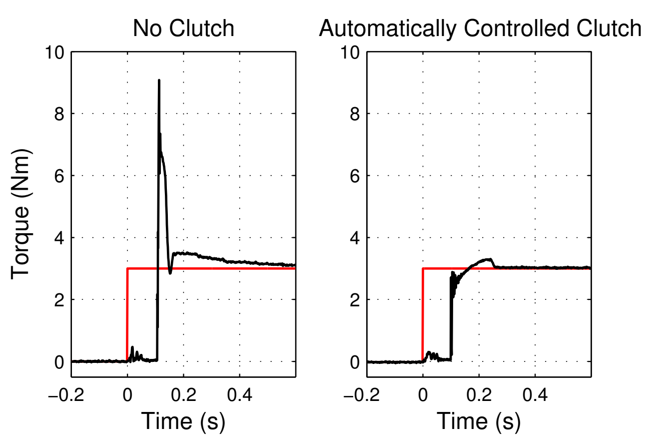

Fig. 12. Automatic Regulation of Coil Current to Track Desired Torque and Minimize Impact Force

impact. Figure 12 shows the resulting torques before, during, and after impact both without the clutch and under automatic clutch control. We see that the clutch activated sufficiently to reach the desired torque level but avoided the larger impact forces experienced in the clutchless actuation case.

D. Telerobotic Implementation

Finally, the telerobotic loop between the master device and the clutch was closed. A user input a motion on the master device intended to test the ability of the SCA to track desired position and force in a telerobotic system, and to demonstrate slow and fast contact with the environment. The user then repeated the motion with the SCA removed. The resulting master and slave position and torque traces from the experiment are shown in Figure 13 and defined in Figure 9. Similar ability to track position and torque are demonstrated, but the large impact forces experienced with the geared DC motor have been lessened by inclusion of the SCA.

VI. Conclusion

We have designed, manufactured, and tested a MR Series Clutch Actuator (SCA) which allows fast physical adjustment of its high-frequency output impedance without sacrificing force tracking bandwidth. The control architecture works with the nonlinear saturation by magnetizing the MRF as necessary, both for autonomous and telerobotic applications. The MR SCA has shown to be an effective coupling for its ease of adjustment and preservation of the transmission dynamics.

Much as a human's ability to vary limb impedance, the actuator's ability to mechanically couple to or decouple from

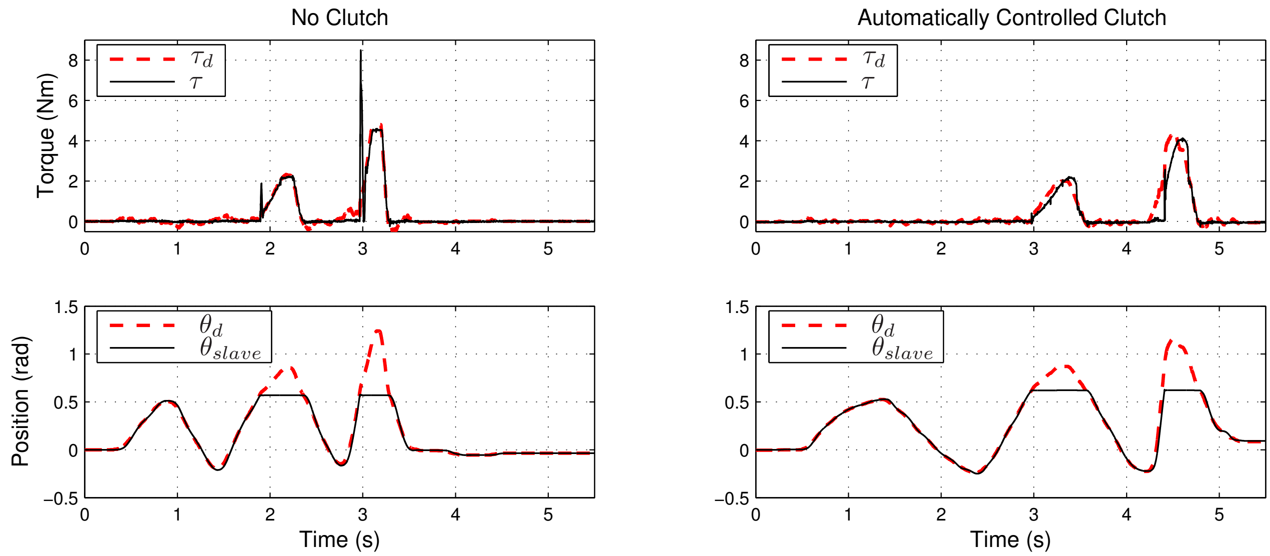

Fig. 13. Telerobotic Activity with SCA in Freespace and in Contact Exhibits Far Smaller Peak Impact Forces

98% of the system inertia creates a large variation in the high-frequency impedance. When desired, this is invaluable in limiting unwanted impact or collision forces at the output. In turn, this can greatly improve device safety, especially in unknown environments or with human contact.

While activation of the MRF in the clutch requires fractions of a second, practical use of the actuator is not hindered. In autonomous use, the clutch can be pre-activated. In telerobotic systems, the torque output is capable of following human commands which are inherently of limited bandwidth. Our experiments confirm good telerobotic position and force tracking while eliminating large collision forces.

In future work, we hope to refine the MR SCA design to reduce overall device size, possibly by employing the MRF in valve mode or adjusting the geometry of the torque transfer plates as the current design is not suited for implementation in the serial kinematics of multi-dof systems. Redesign of the coil, flux path, and amplifiers should allow an increase in the speed of clutch activation changes. We also plan to use the actuator to demonstrate human-like performance in a variety of tasks.

It is our hope that variable impedance actuation will bring greater safety to human-robot interactions and also endow robots with more human-like capabilities, making them more versatile in their expanding applications.

VII. ACKNOWLEDGMENTS

This work was sponsored by an NSF Graduate Research Fellowship and financial support from the Materials Design Institute at Los Alamos National Laboratory. Additionally, we thank Josef Schillig for electromagnetic and mechanical design advice, John Balog for mechanical design advice and manufacturing, and John Brunner for manufacturing efforts.

REFERENCES

[1] M. Zinn, O. Khatib, and B. Roth, "A new actuation approach for human friendly robot design," *ICRA 2004*, no. 1, pp. 249 – 254, 2004.
[2] M. R. Jolly, J. W. Bender, and J. D. Carlson, "Properties and applications of commercial magnetorheological fluids." *J. of Intel. Mat. Sys. and Struct.*, vol. 10, no. 1, pp. 5 – 13, 1999.
[3] G. A. Pratt and M. M. Williamson, "Series elastic actuators," *IROS 1995*, vol. 1, pp. 399 – 406, 1995.
[4] C.-M. Chew, G.-S. Hong, and W. Zhou, "Series damper actuator: a novel force/torque control actuator." vol. 2, pp. 533 – 546, 2004.
[5] R. Van Ham, B. Vanderborght, M. Van Damme, B. Verrelst, and D. Lefeber, "Maccepa, the mechanically adjustable compliance and controllable equilibrium position actuator: Design and implementation in a biped robot," *Robot. Auton. Syst.*, vol. 55, no. 10, pp. 761–768, 2007.
[6] R. Schiavi, G. Grioli, S. Sen, and A. Bicchi, "Vsa-ii: a novel prototype of variable stiffness actuator for safe and performing robots interacting with humans," *ICRA 2008*, pp. 2171–2176, May 2008.
[7] J. W. Hurst, J. Chestnutt, and A. Rizzi, "An actuator with mechanically adjustable series compliance," Robotics Institute, Carnegie Mellon University, Pittsburgh, PA, Tech. Rep. CMU-RI-TR-04-24, Apr. 2004.
[8] H. Herr and A. Wilkenfeld, "User-adaptive control of a magnetorheological prosthetic knee." *Ind. Robot*, vol. 30, no. 1, pp. 42 – 55, 2003.
[9] J. D. Carlson, W. Matthis, and J. R. Toscano, "Smart prosthetics based on magnetorheological fluids." *Proc. of the SPIE - The Int'l Soc. for Opt. Engr.*, vol. 4332, pp. 308 – 316, 2001.
[10] S.-S. Yoon, S. Kang, S.-J. Kim, Y.-H. Kim, M. Kim, and C.-W. Lee, "Safe arm with mr-based passive compliant joints and visco-elastic covering for service robot applications," *IROS 2003*, vol. 3, pp. 2191–2196 vol.3, Oct. 2003.
[11] T. Saito and H. Ikeda, "Development of normally closed type of magnetorheological clutch and its application to safe torque control system of human-collaborative robot," *J. of Intel. Mat. Sys. and Struct.*, vol. 18, no. 12, pp. 1181 – 1185, Dec. 2007.
[12] T. Nakamura, N. Saga, and M. Nakazawa, "Impedance control of a single shaft-type clutch using homogeneous electrorheological fluid," *J. of Intel. Mat. Sys. and Struct.*, vol. 13, no. 7-8, pp. 465 – 469, 2002.
[13] N. Takesue, H. Asaoka, J. Lin, M. Sakaguchi, G. Zhang, and J. Furusho, "Development and experiments of actuator using mr fluid," *IECON 2000*, vol. 3, pp. 1838 – 1843, 2000.
[14] B. M. Kavlicoglu, F. Gordaninejad, C. A. Evrensel, N. Cobanoglu, Y. Liu, A. Fuchs, and G. Korol, "A high-torque magneto-rheological fluid clutch." *Proc. of the SPIE - The Int'l Soc. for Opt. Engr.*, vol. 4697, pp. 393 – 400, 2002.
[15] R. W. Phillips, "Engineering applications of fluids with a variable yield stress," Ph.D. dissertation, UC Berkeley, 1969.